Photoresponse Characteristics of Ppy/Ag_2O Nanocomposites Synthesized by Hydrothermal Method

Zainab S. Ali [1]
Najat A. Dahham [2]

[1] *Department of Physics, College of Science, University of Tikrit, Tikrit, IRAQ*
[2] *Department of Physics, College of Education, Tuzkhurmatu, University of Tikrit, Tuzkhurmatu, IRAQ*

Polypyrrole (Ppy) and Ppy/silver oxide (Ag_2O) nanoparticles (NPs) have been synthesized utilizing hydrothermal method. Then, the pure Ppy and its nanocomposites films with various volume percentages of Ag_2O (10, 30 and 50 vol.%) films were deposited successfully using drop-coat method on glass and Si substrate. The morphology, structural and optical properties of the as-prepared films were measured and characterized utilizing FE-SEM/EDX, XRD, FTIR, and UV. further, these Ppy/Ag_2O nanocomposites were tested to study their influence of Photoresponse properties The photo-detector fabricated employing the Ppy/ Ag_2O-50% showed a good photo-sensitivity of 265.45% and a high responsivity of 243.33 mA/W under the light (532 nm) illumination at bias voltage 5 volt with the rise/decay times of 0.81 sec and 0.85 sec, respectively. The obtained results are proposing that the Ppy/ Ag_2O nanocomposite is a promising material for optoelectronic applications.

Keywords: Ppy/Ag_2O; Hydrothermal method; Drop casting; Photoresponse
Received: 17 January 2024; **Revised:** 15 February, **Accepted:** 22 February 2024

1. Introduction

In today's world, there is a high request for developed opto-electronic devices for everyday life, research organizations, industries, and education field, etc. [1-3]. As significant devices, photodetector (PDs) are fundamental tools in optoelectronic circuits and memory storage, as well as in light-wave communications, and high resolution imaging methods [4]. In the last few years, aromatic conducting polymers (CP) , particularly electro-active polymers, have gotten much explore thought for utilize as advance materials due to their special physical characteristics, However, Conducting polymers, excite an wide interest among researchers due to their interesting optical, electronic, magnetic properties[5-7]. The detection of conducting polymers led to their wide range of applications are in photo-detectors , batteries , solar cells, acoustic wave devices, , nano-generator, UV-nanolaser, varistors, etc. [8]. Among conductive polymers, Polypyrrole (PPy), is one of most extensively investigated polymers, possessing a wide potential application due to its facile, low-cost synthesis, thermal and air stability, good environmental stability, high conductivity [9-11]. In recent years, various types of photo-sensors have been developed by mixing inorganic nano-materials (semi-conductor type) with Conducting polymer, such as PPy/semiconductor -based nano-composites photodetectors, Ppy/TiO_2 [12], Ppy/WO_3 [13], Ppy/CdS [14] Ppy/SnO_2 , etc [15]. silver oxide (Ag_2O) as a perfect p-type has narrow band gap (1.2eV) semiconductor material, is a suitable candidate [16]. Recently, Ag_2O nano-particles have received great attention because of their use for most industrial applications such as for photodetector, photovoltaic cells, storage devices, photodiodes, antibacterial coatings and so on [17]. Here, the advantage of this work is the synthesis of Ppy/Ag_2O nanocomposites for photo-sensing application. The optical, morphological, structural, and photoresponse properties of prepared thin films of Ppy nanotubes and Ppy/Ag_2O nanocomposites have been investigated.

2. Experimental:

Pure Ppy was synthesized employed by hydrothermal method. In this procedure, 0.167g of pyrrole solution and 0.041g of methyl orange acid were dissolved in 50 ml of DI water. Then, 0.675 g of iron (III) chloride was dispersed in 50 ml of DI water and then added it into the above solution with continuous stirring for 10 min in RT. After that, this mixture was transferred into a Teflon lined (autoclave) with heated for 5 h at 150 °C. Then precipitated solution was filtered and the remains obtained was washed several times by DI water and ethanol, alternatively. Further, the definitive product was dried for 3 h in the oven at 70 °C to get Ppy powder. The Ppy powder was dispersed in 15 ml of ethanol utilized the ultrasonic curing for 3 h and it's deposited via drop-casting technique on cleaned glass and Si substrate to make of Ppy thin film.

Ag_2O NPs was synthesized utilized via hydrothermal method. In this step, 0.849 g of silver nitrate was dissolved in 50 ml of DI water. Thereafter, 50 mL of a sodium hydroxide (0.5M) aqueous solution was added drop-wise, with continuous

stirring for 10 min in RT. Then, the mixture solution was moved into a Teflon lined (autoclave) with heated for 5 h at 150 °C. After that, precipitated solution was filtered and the remains obtained was washed several times by DI water and ethanol, alternatively. Further, the definitive product was dried for 3 h in the oven at 100 °C to get Ag_2O NPs. The Ag_2O powder was dispersed in 15 ml of ethanol utilized the ultrasonic curing for 3 h and it's mixed with Ppy solution to form Ppy /Ag_2O Nano-composites with various volume percentages of Ag_2O (10,30 and 50Vol.%), and deposited successfully using drop-coating method on glass and Si substrate to form of Ppy /Ag_2O thin films and labeled as PA-10, PA-30 and PA-50 respectively. The prepared films were examined using Fourier transform-infrared spectroscopy (FT-IR), X-ray diffraction (XRD) Field emission-scanning electron microscopy (FE-SEM), Energy-dispersive X-ray spectroscopy (EDX) and optical spectroscopy. For photodetector measurements, two Al electrodes were thermally-evaporated onto a thin film. the current–voltage (I–V) measurements and visible photo-response were recorded under laser light (532 nm) of power density 5 mW/cm^2 employing Source Measure Unit (UT81B).

3. Results and Discussion

The structural investigations of Ppy /Ag_2O thin films were performed by X-ray diffraction and the obtained results were compared with that of PPy film. XRD plot of pure Ppy and Ppy /Ag_2O films with 10, 30 and 50 Vol% of Ag_2O NPs was showed in Fig. 1. For Ppy film, it is clearly noted that the existence of wide peak at 2θ = 22°, referencing the amorphous nature of the polymer. The wide peak produces by X-ray scattering of Ppy chain [18]. in the state of Ppy/Ag_2O thin films, The sharp peaks of Ag_2O NPs were discovered at 2θ=26°, 32°,38°,44°,55°,57°,64°,68°and 77°, which are assigned to the diffraction from (110), (111), (200), (211), (220), (221), (311), (222), and (123) planes of Cubic Ag_2O [19-20]. These peaks are agreed with the JCPDS card no. 76-1393 for Cubic Ag_2O. The difference in average crystallite size of the as-prepared samples were calculated with utilizing Scherer's relation [21]

$$D_{av} = \frac{0.9\,\lambda}{\beta \cos\theta} \qquad (1)$$

where λ is X-ray wavelength(Cu Kα-1.54056 Aº), θ is the diffraction angle, and β is full-width at half-maxima respectively. The measurements showed that the values of average size for PA-10, PA-30 and PA-50 nanocomposites are 35, 37 and 41 nm respectively.

The characteristics of the FTIR spectroscopy for Ppy and their nanocomposites films are demonstrated in the Fig. 2. The main peaks for pure Ppy were observed at 1543, 1483, 1319, 1184, 1037, 964, and 918 cm^{-1}. The peaks at 1543 and 1483cm^{-1} may be ascribed to the C-C and C-N stretching-vibrations in the pyrrole rings, respectively [22]. The band assigned at 1319 cm^{-1} was related of C–H or C–N in-plane deformation modes [23], while the peaks at 1184 and 1037cm^{-1} were related to the breathing-vibrations of the pyrrole rings[24]. In also, the peak related at 964 cm^{-1} correspond to the C–H and N–H in-plane deformation-vibrations [25]. The out-plane bending-vibration of the C-H is assigned at about 918 cm^{-1}[26]. However, some changes of characteristic peaks are observed in Ppy-Ag_2O samples. This shift can be occurred due to the incorporation of Ag_2O within the Ppy structure.

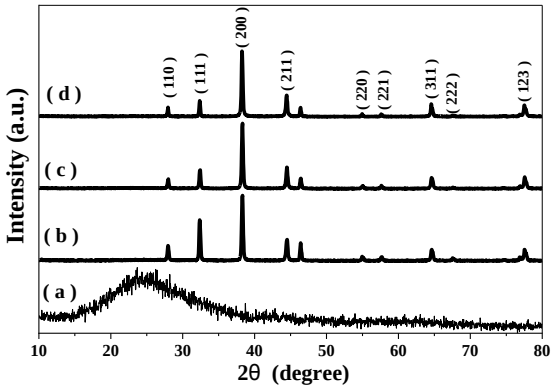

Fig. (1) XRD patterns of (a) Ppy, (b) PA-10, (c) PA-30 and (d) PA-50

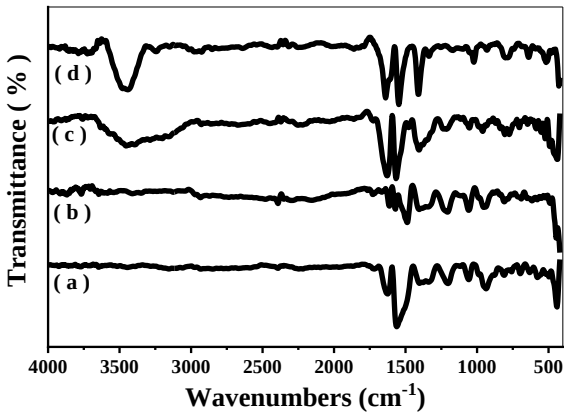

Fig. (2) FTIR spectra of (a) Ppy, (b) PA-10, (c) PA-30 and (d) PA-50

Figure (3) displays the FE-SEM pictures of Ppy and Ppy /Ag_2O nanocomposites films. The FE-SEM picture of pure PANI has a mixture of nanotubular morphology with some irregular globular. Dye-free polypyrrole possess a characteristic spherical shape. However, the presence of Methyl Orange into the polymerization medium leaded to the formation of nanotubular morphology having average particle diameter approximately 100–200 nm, because it works as a morphology-directing factor [27]. The FESEM pictures of Ppy /Ag_2O nanocomposites films Fig. 3(b) to (d) confirmed that Ag_2O NPs were implanted almost fully in the polymer form with average particle diameters approximately 200–400 nm, confirming the preparation of nano-composites, and it's observed that improvement in the

incorporation of Ag_2O NPs to the Ppy form with increasing concentration of Ag_2O. Thus, the outcomes obtained from FESEM analyses which would ease good electrical-conductivity [28].

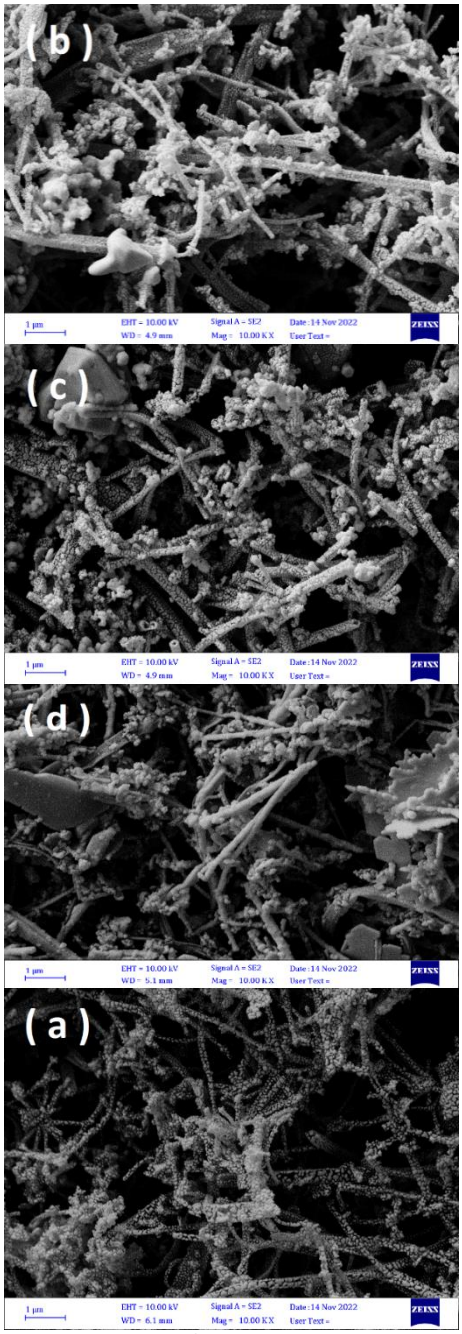

Fig. (3) FE-SEM images of (a) Ppy, (b) PA-10, (c) PA-30 and (d) PA-50

In addition, an elemental analysis of all films was tested via EDX analysis. Figure (4) displays the EDX image of the as-deposited films that confirms the presence of S, C and N in the Ppy film, and also it revealed the existence of Ag and O elements in Ppy/Ag_2O nanocomposites films. The existence of sulfur(S) confirms that MO was integrated in films [29]. The outcomes obtained that confirms in the incorporation of Ag_2O NPs in polymer structure without forming any impurities.

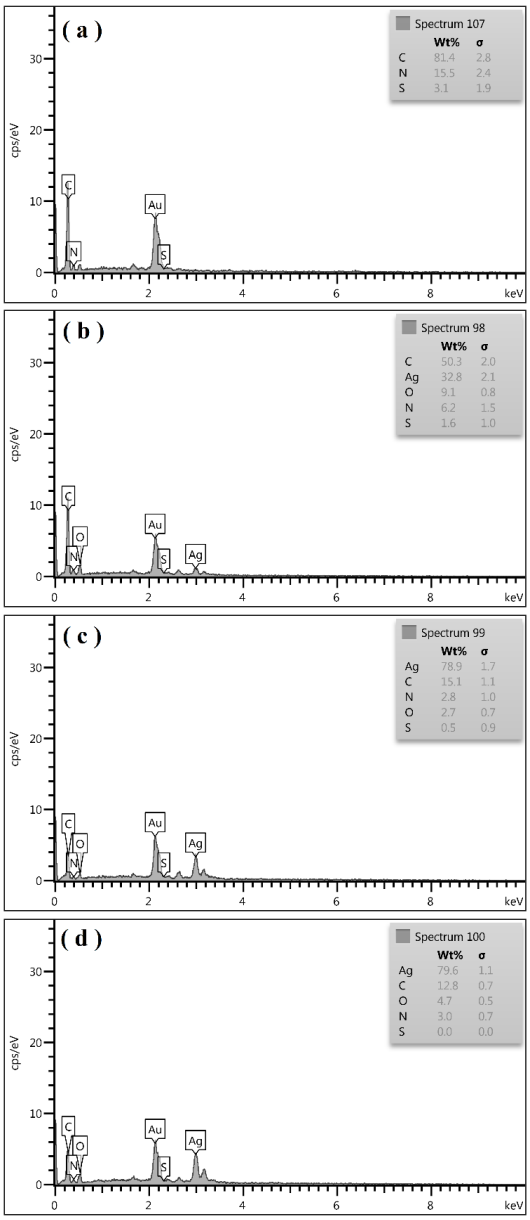

Fig. (4) EDX images of (a) Ppy, (b) PA-10, (c) PA-30 and (d) PA-50

In order that discuss the optical properties of all samples, the UV–Visible absorption spectra and (αhv)2 with hv plots are displayed in Fig. 5 and 6. As is obvious from Fig. 5, the absorbance spectra of Ppy film showed absorption peak at 463 nm associated as being a π–π* transition, with the bi-polaron peak at 970 nm. Compared by Pure Ppy, the nanocomposites films exhibits the π–π* peak is expanded, and red shifted due to the incorporation of Ag_2O NPs in polymer structure with increasing concentration of Ag_2O and also, the bi-polaron peak is expanded, that indicates a change in the conjugation length [30-32].

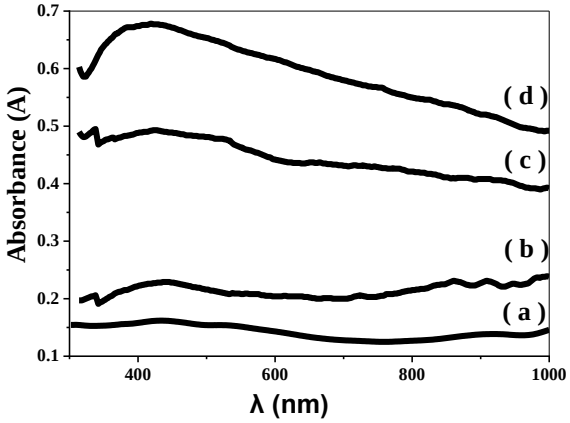

Fig. (5) Absorption spectra of (a) Ppy, (b) PA-10, (c) PA-30 and (d) PA-50

The direct band gap (Eg) of the as-prepared films were obtained by the following relation [33]:

$$(\alpha h\nu) = A(h\nu - Eg)^{\frac{1}{2}} \quad (2)$$

where A, α, ν and h indicate for the constant

A gradual fall of E_g value from 1.63 to 1.46 eV is observed with adding Ag_2O NPs as illustrated in Fig. (6). This decrease in E_g may be due to the increasing in the crystallite size, with increase in Ag_2O NPs.

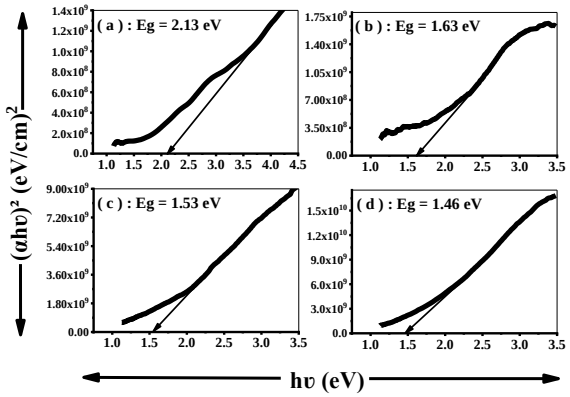

Fig. (6) Plots of $(\alpha h\nu)^2$ with $h\nu$ for (a) Ppy, (b) PA-10, (c) PA-30 and (d) PA-50

The current-voltage (I-V) test of as-fabricated photodetectors were studied in the existence and non-existence of laser light (532 nm) of power density of 5 mW/cm^2 for the potential range between 5V and –5V. Figure (7) displays the I-V plots of the devices measured under dark and visible-light of 5 mW/cm^2 intensity. In light state the value of photocurrent increases significantly when compared to the dark state, due to the generation of an electron-hole pair under illumination.

Figure (8) shows that the Photo-current verses time of all photo-detector. Obviously, all films display higher photocurrent compared to the corresponding dark current under the existence of illumination, which implies the generation of phot-induced electron-hole pair in the films.

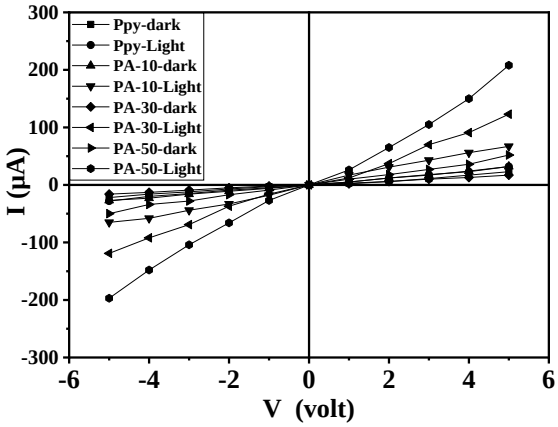

Fig. (7) I-V characteristics of as-fabricated photodetectors

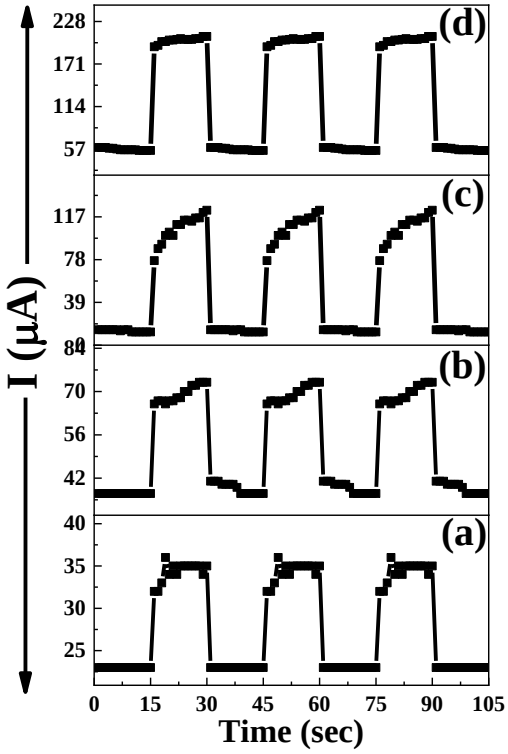

Fig. (8) Variation of photo-current with time for (a) Ppy, (b) PA-10, (c) PA-30 and (d) PA-50.

The three parameters, i.e., sensitivity (S), responsivity (R), and specific detectivity (D*), of the photodetectors are evaluated by the relations [34]:

$$S(\%) = \frac{I_{ph}}{I_{dark}} \times 100 \quad (3)$$

$$R = \frac{I_{ph}}{A.P} \quad (4)$$

$$D = \frac{R.A^{1/2}}{(2 \times e \times I_{dark})^{1/2}} \times 100 \quad (5)$$

where I_{ph} is the photocurrent (I_{ph}=I_{light}−I_{dark}), P is the power of light, A is lighting area and e is electronic-charge

The estimated photodetectors parameters are tabulated in table (1). The as-fabricated device of pure Ppy display a sensitivity of 39.13%, R of 15 mA/W and detectivity of 1.92×10^9 Jones for the illumination intensity of 5 mW/cm^2. The as-fabricated device based on PA-50 exhibits sensitivity as high as,

265.45%, R of 243.33 mA/W and detectivity of 20.09×10^9 Jones. Clearly, the performance of PA-(10, 30 and 50) device enhanced several times with compared to pure Ppy. A compare of the photo-detector performance of the current paper with past photodetectors for Ppy/ metal oxide nanostructures are displayed in table (1). Obviously, these results that the performance of Ppy/Ag_2O photodetector is excellent in several asides of previously reported papers.

The rise time and decay time of as-fabricated photodetectors were evaluated for 1 cycle from Fig. (8). The rise time and fall time of Ppy, PA-10, PA-30 and PA-50 photodetectors are (0.88, 0.85, 1.51 and 0.85 s) and (0.8, 0.83, 0.79 and 0.81 s) respectively. The values of rise/decay time are less than 2 s. Comparison of rise /decay times of as-fabricated photodetectors with other previous works are tabulated in Table 1. From the results, it is shown that Ppy/$Ag_2$0 nanocomposite are a promising component for next-generation visible-light photodetection devices.

4. Conclusions

In this article, Polypyrrole NTs and Ag_2O NPs have been successfully prepared employing hydrothermal method, Also, it studied the effect of adding Ag_2O NPs with different mixing ratios (10, 30, and 50 vol.%) on the physical properties of Ppy thin films prepared employing drop-casting. The XRD analysis displayed the amorphous structure of Ppy film and the formation of cubic structure of Ppy /Ag_2O films. FE-SEM analysis showed the nanocrystalline nature by formation of a mixture of nanotubular and globular morphology. The improvement in the direct band-gap value from 2.13 eV for pure Ppy to 1.46 eV for Ppy/Ag_2O-50%. The photo-detector fabricated of Ppy/Ag_2O-50% showed a good photo-sensitivity of 265.45% and high responsivity of 243.33 mA/W at 5 V applied bias with rise time and decay times < 2s.

References

[1] I.L.P. Raj et al., "Enhancement of photo-sensing properties of CdS thin films by changing spray solution volume", *Sens. Actuat. A: Phys.*, 315 (2020) 112306.

[2] C.M. Lieber, "Nanoscale science and technology: building a big future from small things", *MRS Bull.*, 28(7) (2003) 486-491.

[3] Y. Jung, D.K. Ko and R. Agarwal, "Synthesis and structural characterization of single-crystalline branched nanowire heterostructures", *Nano Lett.*, 7(2) (2007) 264-268.

[4] T. Zhai et al., "Fabrication of high-quality In_2Se_3 nanowire arrays toward high-performance visible-light photodetectors", *ACS Nano*, 4(3) (2010)1596-1602.

[5] B.H. Kim et al., "Synthesis, characteristics, and field emission of doped and de-doped polypyrrole, polyaniline, poly (3,4-ethylenedioxythiophene) nanotubes and nanowires", *Synth. Met.*, 150(3) (2005) 279-284.

[6] M.R. Mahmoudian, Y. Alias and W.J. Basirun, "Electrodeposition of (pyrrole-co-phenol) on steel surfaces in mixed electrolytes of oxalic acid and DBSA", *Mater. Chem. Phys.*, 124(2-3) (2010) 1022-1028.

[7] A. Asan, M. Kabasakaloglu and M.L. Aksu, "The role of oxalate ions in the coverage of mild steel with polypyrrole", *Russian J. Electrochem.*, 41(2) (2005) 154-158.

[8] F. Kanwal et al., "Synthesis of polypyrrole–ferric oxide (Ppy–Fe_2O_3) composites and study of their structural and conducting properties", *Synth. Met.*, 161(3-4) (2011) 335-339.

[9] Y. Li et al., "Polypyrrole prepared in the presence of methyl orange and ethyl orange: nanotubes versus globules in conductivity enhancement", *J. Mater. Chem. C*, 5(17) (2017) 4236-4245.

[10] J. Huang et al., "Ultrasound assisted polymerization for synthesis of ZnO/Polypyrrole composites for zinc/nickel rechargeable battery", *J. Power Sourc.*, 271 (2014) 143-151.

[11] E. Alekseeva et al., "The composites of silver with globular or nanotubular polypyrrole: the control of silver content", *Synth. Met.*, 209 (2015) 105-111.

[12] W. Zheng et al., "Fabrication of a visible light detector based on a coaxial polypyrrole/TiO_2 nanorod heterojunction", *RSC Adv.*, 4(85) (2014) 44868-44871.

[13] B. Gowtham et al., "Upliftment the rectification behavior of PPy-WO_3 nanocomposites for photodetector applications", *Inorg. Chem. Commun.*, 135 (2022) 109105.

[14] M. Amiri and N. Alizadeh, "Mid-infrared photoconductivity of polypyrrole doped with cadmium sulfide quantum dots", *J. Phys. Chem. Solids*, 141 (2020) 109383.

[15] S. Fu et al., "Deep Ultraviolet Photodetector with Ultrahigh Responsivity based on a Nitrogen-Doped Graphene-Modified Polypyrrole/SnO_2 Organic/Inorganic p–n Heterojunction", *Adv. Mater. Interfac.*, 10 (2023) 2202488.

[16] A.C. Nwanya et al., "Structural and optical properties of chemical bath deposited silver oxide thin films: Role of deposition time", *Adv. Mater. Sci. Eng.*, 2013 (2013) 1-8.

[17] A. Umar et al., "Enhanced NO_2 gas sensor device based on supramolecularly assembled polyaniline/silver oxide/graphene oxide composites", *Ceram. Int.*, 47(18) (2021) 25696-25707.

[18] A. Elahi et al., "Polypyrrole and its nanocomposites with $Zn_{0.5}Ni_{0.4}Cr_{0.1}Fe_2O_4$ ferrite: preparation and electromagnetic properties", *J. Mater. Sci.: Mater. Electron.*, 27 (2016) 6964-6973.

[19] J. Fowsiya and G. Madhumitha, "Biomolecules derived from Carissa edulis for the microwave assisted synthesis of Ag_2O nanoparticles: A study against *S. incertulas*, *C. medinalis* and *S. Mauritia*", *J. Cluster Sci.*, 30 (2019) 1243-1252.

[20] A. Ananth, R.H. Jeong and J.H. Boo, "Preparation, characterization and CO oxidation performance of Ag_2O/γ-Al_2O_3 and (Ag_2O+ RuO_2)/γ-Al_2O_3 catalysts", *Surfaces*, 3(2) (2020) 251-264.

[21] B.D. Cullity, **"Elements of X-ray Diffraction"**, Addison-Wesley Publishing (Boston, 1956), Ch. 9, p. 259.

[22] R. Moučka et al., "One-dimensional nanostructures of polypyrrole for shielding of electromagnetic interference in the microwave region", *Int. J. Mol. Sci.*, 21(22) (2020) 8814.
[23] J. Stejskal et al., "Polypyrrole salts and bases: superior conductivity of nanotubes and their stability towards the loss of conductivity by deprotonation", *RSC Adv.*, 6(91) (2016) 88382-88391.
[24] J. Kopecká et al., "Polypyrrole nanotubes: mechanism of formation", *RSC Adv.*, 4(4) (2014) 1551-1558.
[25] A. Munteanu et al., "Bidisperse magnetorheological fluids utilizing composite polypyrrole nanotubes/magnetite nanoparticles and carbonyl iron microspheres", *Rheologica Acta*, 62(9) (2023) 461-472.
[26] D. Kopecký et al., "Optimization routes for high electrical conductivity of polypyrrole nanotubes prepared in presence of methyl orange", *Synth. Met.*, 230 (2017) 89-96.
[27] M. Varga et al., "The ageing of polypyrrole nanotubes synthesized with methyl orange", *Euro. Polym. J.*, 96 (2017) 176-189.
[28] I. Sapurina et al., "Polypyrrole nanotubes: the tuning of morphology and conductivity", *Polymer*, 113 (2017) 247-258.
[29] Y. Li et al., "Polypyrrole prepared in the presence of methyl orange and ethyl orange: nanotubes versus globules in conductivity enhancement", *J. Mater. Chem. C*, 5(17) (2017) 4236-4245.
[30] Y. Liu et al., "Preparation of PPy/TiO_2 core-shell nanorods film and its photocathodic protection for 304 stainless steel under visible light", *Mater. Res. Bull.*, 124 (2020) 110751.
[31] M. Rahaman et al., "Chemical and electrochemical synthesis of polypyrrole using carrageenan as a dopant: Polypyrrole/MWCNT nanocomposites", *Polymers*, 10(6) (2018) 632.
[32] M. Trchová and J. Stejskal, "Resonance Raman spectroscopy of conducting polypyrrole nanotubes: disordered surface versus ordered body", *J. Phys. Chem. A*, 122(48) (2018) 9298-9306.
[33] O. Stenz, **"The Physics of Thin Film Optical Spectra"**, Springer (2005), Ch. 6, p. 301.
[34] S. Pyshkin and J. Ballato, **"Optoelectronics: Advanced Device Structures"**, BoD–Books on Demand .l, (2017), Ch. 12, p.257.
[35] S.K. Singh and R.K. Shukla, "Optical and photoconductivity properties of pure Polypyrrole and titanium dioxide-doped Polypyrrole nanocomposites", *Mater. Sci. Semicond. Process.*, 31 (2015) 245-250.
[36] L. Zheng et al., "Scalable-production, self-powered TiO_2 nanowell–organic hybrid UV photodetectors with tunable performances", *ACS Appl. Mater. Interfaces*, 8(49) (2016) 33924-33932.
[37] H. Chen et al., "Ultrasensitive self-powered solar-blind deep-ultraviolet photodetector based on all-solid-state polyaniline/MgZnO bilayer", *Small*, 12(42) (2016) 5809-5816.
[38] M. Amiri and N. Alizadeh, "Highly photosensitive near infrared photodetector based on polypyrrole nanoparticle incorporated with CdS quantum dots", *Mater. Sci. Semicond. Process.*, 111 (2020) 104964.
[39] O.A. Kareem, I.M. Ibrahim and S.J. Mohameed, "Optimizing the optical response of polypyrrol nanofibers by decoration with ZnO nanoparticles", *AIP Conf. Proc.*, 2400(1) (2022) 030008.
[40] A.M. Elsayed et al., "Highly Uniform Spherical MoO_2-MoO_3/Polypyrrole Core-Shell Nanocomposite as an Optoelectronic Photodetector in UV, Vis, and IR Domains", *Micromachines*, 14(9) (2023) 1694.
[41] A. Ben Gouider Trabelsi et al., "Photodetector-Based Material from a Highly Sensitive Free-Standing Graphene Oxide/Polypyrrole Nanocomposite", *Coatings*, 13(7) (2023) 1198.
[42] M. Rabia et al., "Porous-Spherical Cr_2O_3-Cr (OH) 3-Polypyrrole/Polypyrrole Nanocomposite Thin-Film Photodetector and Solar Cell Applications", *Coatings*, 13(7) (2023) 1240.

Table (1) The Photodetector parameters of Ppy and Ppy/Ag_2O nanocomposites thin films when compared to other previous works

Photodetector	Wavelength (nm)	Bias (V)	S (%)	R (mA/W)	D (Jones)	Rise Time (s)	Fall Time (s)	Refs
Ppy/TiO_2	365	-	1.17	-	-	273	253	[35]
Polyaniline/ TiO_2	320	5	-	3×10^{-3}	-	-	-	[36]
Polyaniline/ MgZnO	250	5	-	0.1	-	-	-	[37]
Ppy/CdS	850	10	120	3.8	2.1×10^{16}	-	-	[38]
Ppy/ZnO	720	-	167.4	-	-	2.5	3	[39]
Ppy/ MoO_2, MoO_3	540	2	-	4	5.85×10^{8}	-	-	[40]
Ppy/GO	540	2	-	0.31	6.9×10^{7}	-	-	[41]
Ppy/Cr_2O_3	540	3	-	0.0143	3.21×10^{6}	-	-	[42]
Ppy	532	5		39.13	15	0.8	0.88	This work
PA-10				83.78	51.67	0.83	0.85	
PA-30				733.33	146.67	0.79	1.51	
PA-50				265.45	243.33	0.81	0.85	

